

LA-UR- 93-3557

Title: DETECTION OF MINING EXPLOSIONS USING IONOSPHERIC
TECHNIQUES

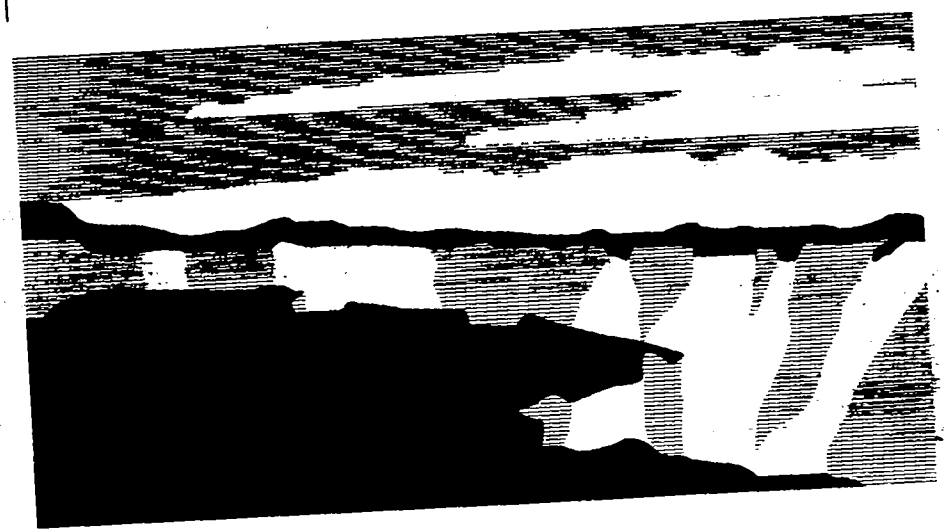
Author(s): T. JOSPEH FITZGERALD

Submitted to: DEPARTMENT OF ENERGY HEADQUARTERS

DO NOT CIRCULATE

PERMANENT RETENTION

LOS ALAMOS NATIONAL LABORATORY
3 9338 00202 5699



Los Alamos
NATIONAL LABORATORY

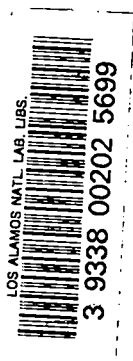
Los Alamos National Laboratory, an affirmative action/equal opportunity employer, is operated by the University of California for the U.S. Department of Energy under contract W-7405-ENG-36. By acceptance of this article, the publisher recognizes that the U.S. Government retains a nonexclusive, royalty-free license to publish or reproduce the published form of this contribution, or to allow others to do so, for U.S. Government purposes. The Los Alamos National Laboratory requests that the publisher identify this article as work performed under the auspices of the U.S. Department of Energy.

Detection of Mining Explosions Using Ionospheric Techniques.

T. Joseph Fitzgerald

Los Alamos National Laboratory, Los Alamos, New Mexico 87545

September 24, 1993



Contents

Abstract	3
1 Introduction	4
2 Airblast from mining explosions	6
3 Results	9
3.1 <i>Measurement Technique</i>	9
3.2 <i>Morenci Copper Mine</i>	13
3.3 <i>San Juan Coal Mine</i>	17
4 Discussion	18
4.1 <i>Detectability of Mining Explosions</i>	18
4.2 <i>System Concepts</i>	21
5 Conclusion	22
6 Acknowledgement	24
7 References	24

Abstract

An evader wishing to circumvent a low-yield or comprehensive nuclear test ban treaty or the Non-Proliferation Treaty may decouple a nuclear test in an underground cavity producing a weak seismic signal that would be erroneously interpreted as a mining explosion. Since hundreds of surface mining explosions with seismic magnitudes similar to those expected from decoupled low-yield nuclear tests are conducted each day treaty verification becomes an enormous discrimination task. An additional means of discrimination between mining explosions and underground nuclear tests would be to detect acoustic waves produced by airblast; for a given seismic magnitude the airblast produced by a surface mining explosion has about ten times the energy content as that produced by a contained underground explosion. These acoustic waves propagate vertically into the upper atmosphere where they interact with the ambient plasma of the ionosphere to produce effects that are detectable using radio remote-sensing techniques. For a contained underground explosion, surface ground motion near ground zero produces the airblast; Los Alamos National Laboratory has detected acoustic waves in the ionosphere at ranges up to 100 km from such sources. Surface mining explosions produce airblast from a combination of earth motion, venting, gas escape, and surface seismic waves. In this report we review the phenomenology of airblast from mining explosions and describe recent detections of mining explosions using radio techniques to remotely sense the ionosphere directly above the mine.

1 Introduction

The occurrence rate of seismic events increases with decreasing seismic magnitude; historically, in the regime of the 150 kt Threshold Test Ban Treaty, earthquakes with seismic magnitude $m_b > 3.5$ were the chief concern for discrimination of clandestine nuclear tests. Although a difficult task, teleseismic detection and discrimination of underground nuclear explosions and earthquakes has made considerable progress for the limited number of events in this magnitude range. In the future, in a regime of a low-yield or comprehensive test ban, detection and discrimination must be extended to a lower magnitude with a concomitant increase in events. Such events, which must be detected at regional ranges, will have local magnitudes, m_L , as low as 2.0. Rather than being limited to earthquakes, many of these events will be produced by commercial mining explosions. Much research has been devoted to the discrimination of mining explosions; attention has been concentrated on signal modulation effects caused by the ripple firing used to decrease ground vibration and air blast. Other discriminants that are under consideration is similarity in location and waveform to previous explosions, time-of-day, etc.

Richards et al. [1992] have discussed the question of seismic discrimination of mining blasts using activity in the United States as an example. They estimate that there are about 30 large explosions (>50 t) per day in the U. S.; on average one of these large explosions will be greater than 200 t. There are about 200 medium explosions (5–50 t) per day. *Richards et al.* state

If the concern is with identifying all nuclear explosions down to about 5 kt, the intersection with industrial chemical explosions appears manageable if there is a will to take a problem-solving approach to the limited number of evasion scenarios, such as decoupling. If the concern is with monitoring down to 1 kt, i.e., at yield levels low enough that full decoupling becomes technically more feasible (with decoupling factors around 70 at frequencies below the corner frequency), then monitoring would require a threshold of detection low enough that many thousands of chemical explosions would be routinely recorded. In this situation, the key to robust methods of discrimination will be an understanding of the signals of ripple-fired explosions, as opposed to single-shot explosions. Amplitudes of regional seismic waves are much reduced by ripple firing.

Their intersection point is vague, but it appears that a decoupled 5 kt nuclear explosion needs to be discriminated from a 50 t mining explosion.

Most of these large mining explosions occur at surface pits; thus, some fraction of the explosion energy is released into the atmosphere as airblast. This fraction is small because the explosion is designed to pulverize rock while keeping ground vibration and airblast to a minimum to prevent complaints from nearby population. However, the lower atmosphere is an excellent transmission medium for acoustic waves with periods of ~ 1 second or more; moreover, the relative amplitude of vertically

propagating acoustic waves increases exponentially with height. Such acoustic waves interact with ambient plasma at altitudes of 100 km or more (the ionosphere) to produce changes in electron density which are detectable because of the induced change in the index of refraction of radio waves propagating through the plasma. Los Alamos National Laboratory has conducted extensive experiments to detect the acoustic signature of sources such as underground nuclear tests, earthquakes, and surface conventional explosions in the ionosphere. Measurements conducted by the Ionospheric Physics group indicate that surface conventional explosions with yields as low as 150 kg may be detected in the ionosphere above the source. A number of remote sensing techniques were developed to employ radio transmissions to detect the signatures at regional ranges of 500-1000 km. These measurements indicate that the different types of sources produce ionospheric signatures which differ in form, extent, or strength and thus may be discriminated. We expect that a mining explosion would produce a much larger ionospheric signature than a contained underground explosion with the same seismic magnitude. This difference in signature could be used to determine if the airblast accompanying a seismic event was consistent with a mining explosion source.

The current research project, Explosion Discrimination using Ionospheric Techniques (EDIT), is related to and builds on previous and current research at Los Alamos but may be distinguished in its aims. The Ionospheric Monitoring Program (IMP) developed techniques to detect the acoustic signature produced by surface ground motion above an underground nuclear explosion and to relate the magnitude of the ionospheric signature to the yield of the explosion. The IMP also investigated the signature of earthquakes in the ionosphere. The IMP was aimed at developing a system to conduct monitoring of the Threshold Test Ban Treaty on a global scale. The Regional Ionospheric Monitoring System (RIMS) was a short lived program to develop techniques to monitor limited geographic areas in support of the Non-Proliferation Treaty and a possible Comprehensive Test Ban Treaty. Current ionospheric work in the Source Region Program is aimed at relating the acoustic disturbance to ground motion and thus to properties of the geology near an underground nuclear explosion. These programs have in common the detection of the acoustic pulse in the ionosphere near the source where the signal is strongest using remote sensing techniques. This may be distinguished from the ROSTER program which aims to detect the ionospheric signature of acoustic waves at remote locations and attempts a global coverage; it is also directed at the detection of large surface explosions. The Infrasound program also aims to detect acoustic signatures at remote locations using ground based instruments directly sensitive to air pressure variations. Both these current programs may be able to contribute to the discrimination of mining explosions. However, it is likely that the techniques used in the EDIT program are at least as sensitive as those employed by ROSTER and Infrasound and these programs have not up to this time addressed the issue of the discrimination of mining explosions. Therefore the EDIT program does not duplicate the work currently being conducted by ROSTER and Infrasound and will contribute to the overall goals of these programs.

Ionospheric discrimination of mining explosions would be based on the idea that there would be an ionospheric signature accompanying a mining explosion which would not be present for an underground nuclear explosion. Suppose that there is a detectable ionospheric signature accompanying mining explosions of seismic magnitude greater than m_r , corresponding to the intersection noted by *Richards et al.* [1992]. Suppose also that the ionospheric signature of an underground nuclear test (UGT) may be detected only down to a magnitude of m_i where $m_i > m_r$; then there is a range of magnitudes for which mining explosions would generate ionospheric signatures while UGT's would not. If a questionable seismic event generated an ionospheric disturbance we could confirm the likelihood that it was a mining explosion; on the other hand, if it was not accompanied by an ionospheric signature it would be suspect.

The major research issues of the first year of the EDIT project concerned the production and the extent of ionospheric perturbations produced by mining explosions. To that end we have examined local measurements of airblast conducted by the U. S. Bureau of Mines. We have also conducted a series of ionospheric measurements in conjunction with mining explosions and have successfully detected an ionospheric signature for four of these events. In this report we discuss these measurements and interpret them in relation to the research objectives.

2 Airblast from mining explosions

The airblast phenomenology of surface mining explosions is intermediate between unconfined explosions and contained underground explosions. Figure 1 shows the time development of a typical mining explosion from a single drill hole [*Morhard, 1987*]. The purpose of the explosion is to pulverize the rock adjacent to the drill hole and move it to the lower bench so that it can be removed for processing if it contains desirable minerals or so that it can be stripped away from underlying levels that contain valuable material as in coal mining. Typically there would be a number of these individual explosions in a blast with a delay between them (ripple firing) to produce the optimum pulverization and movement while limiting undesirable ground motion. The depth of the drill hole is about equal to the height of the bench which is typically about 18 m. The explosive, usually an ammonium nitrate-fuel oil (ANFO) mix, fills the bottom two-thirds of the drill hole; stemming material, designed to confine the explosion, fills the top third. The detonation starts at the bottom of the hole. Figure 1 illustrates the horizontal slumping motion of the face, the vertical uplift of the top surface, and the ejection of the stemming material. These motions together with gas escaping through the fractured rock and acoustic waves generated by seismic waves all contribute to airblast. Thus there are four contributions to airblast: (1) air pressure pulse from rock displacement at the face or at the borehole collar; (2) stemming release pulse from the ejection of the stemming material; (3) gas release pulse from escape gases; (4) rock pressure pulse from the vibrating surface [*Siskind, et al., 1980*]. For comparison, the air pressure pulse from a contained underground

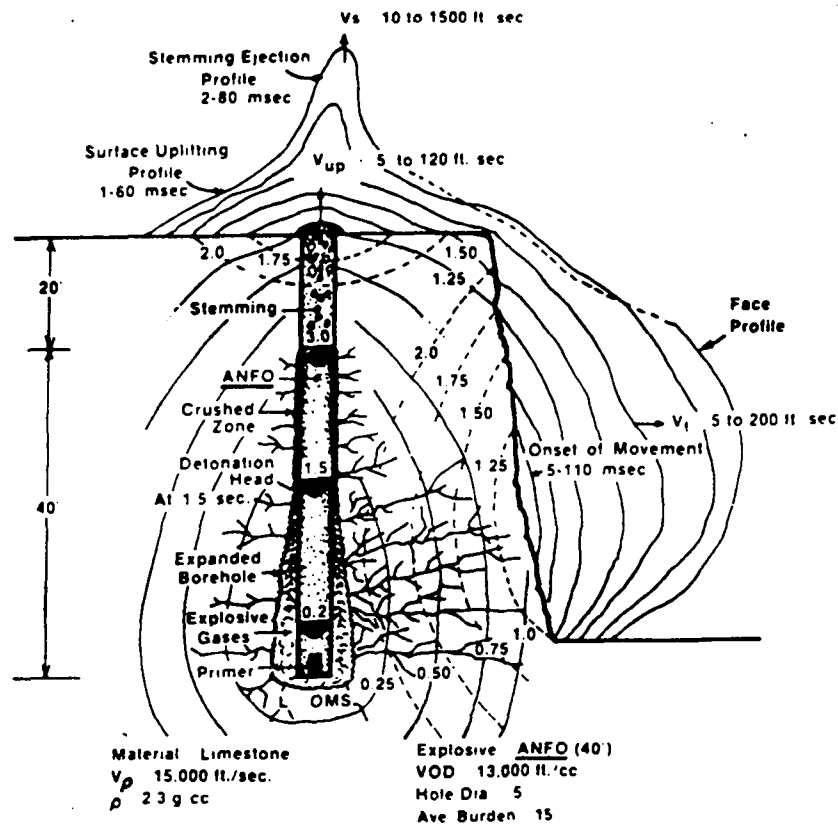


Figure 1: Diagram of the time development of a typical mining explosion. The ANFO explosive is ignited at the bottom of the borehole. The face slumps to the right while top surface is lifted. The stemming material is ejected vertically [Morhard,1987].

explosion arises chiefly from rock displacement at the surface above the explosion and is analogous to the air pressure pulse generated near the blast hole collar; face motion is not present. A rock pressure pulse from surface seismic waves radiating away from ground zero has also been observed following underground explosions. On the other hand, neither a gas or a stemming release pulse would occur for a well-contained underground explosion.

The U. S. Bureau of Mines has conducted extensive measurements of airblast from mining explosions; these measurements were conducted to form a database that could be used to guide operators in limiting overpressures at buildings adjacent to mines. The pressure sensors were placed near ground level at horizontal ranges of less than a few km from the explosion. The measured airblasts showed a great deal of variability related to differences in confinement, type of mine, type of shot, geology, and weather conditions [Siskind, et al., 1980]. Weather affects the overpressure at the ground surface because the usual decrease of air temperature with altitude refracts acoustic waves upward away from the surface; thus variations in temperature will cause variations in measured overpressure. This variation will be reduced for acoustic waves propagating vertically into the upper atmosphere. Figure 2 shows a scatter plot of measured peak overpressure versus cube-root scaled range for a wide variety

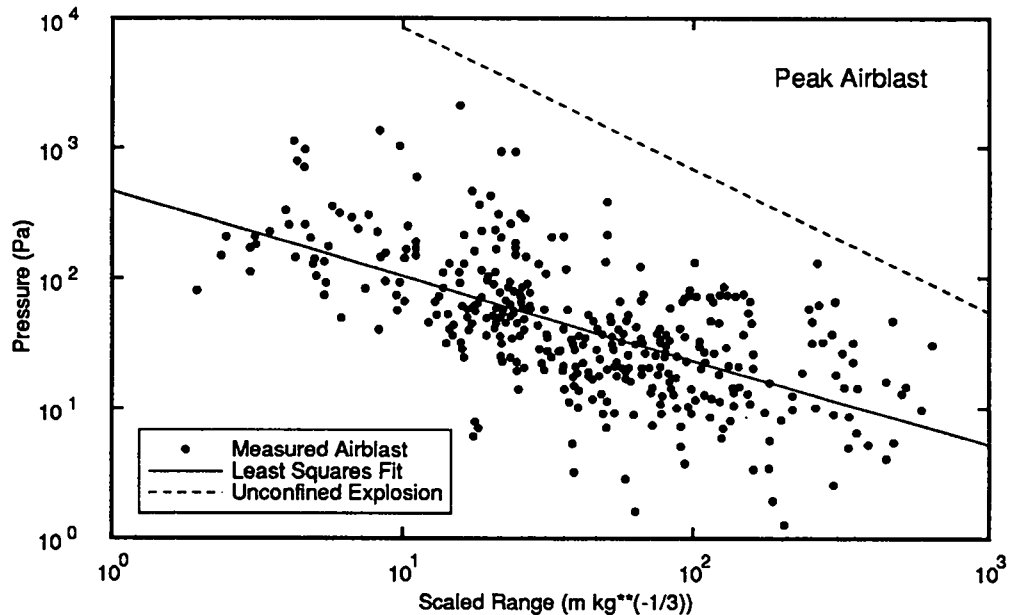


Figure 2: Scatter plot of measured peak pressure versus scaled range for a variety of mining explosions [Siskind, 1990]. The line labelled *Unconfined* indicates the predicted overpressure for a free-air HE detonation. Also shown is a least-squares fit to the measurements. The preponderance of the measurements show a peak airblast amplitude of about 2.5% of that expected for an unconfined explosion

of mining explosions [Siskind, 1990]. Most of these points represent small explosions; that is, 84% had a total charge of less than 10 t and 95% had a total charge of less than 50 t. The line labelled *Unconfined* indicates the predicted overpressure for a free-air detonation of high explosive (HE). The preponderance of the measurements show a peak airblast amplitude of about 2.5% of that expected for an unconfined explosion; in terms of energy release, this would represent confinement by a factor of 1600. As indicated by the least squares fit through the measurements, there is a tendency for the the confinement factor to decrease at large scaled ranges.

We can interpret these measurements in terms of the acoustic energy content of the measured wave forms. Figure 3 shows three sample airblast measurements for shots labelled 48, 86, and 147; the total charge for these shots were 10.3, 13.0, and 262 t [Siskind, et al., 1980]. The measured peak overpressures were 20 Pa at 741 m range, 112 Pa at 218 m, and 71 Pa at 2100 m. The pressure history for shot 86 which was measured at relatively close range shows much high frequency content arising from the 12 individual detonations. Shot 47 which was measured at greater range shows the early arrival of low amplitude fluctuations caused by the rock pressure pulse followed later by airblast from the sources at the explosions: rock displacement, stemming release, etc. Little high frequency content remains in the airblast at this range even

though there were eight individual explosions. Shot 147 was measured at even greater range and shows chiefly a leading overpressure followed by an underpressure with little high frequency content; there were 60 individual shots making up the total explosion.

The acoustic energy density of a plane wave is given by $p^2/\rho c^2$ where p is the pressure perturbation, ρ is the air density, and c is the sound speed. One can obtain a crude estimate of the energy flux by assuming that the waveform does not change in time and that the range is great enough that the a plane wave approximation is adequate. Integrating over the waveforms shown in Figure 3 gives the following energy flux: 0.20, 2.6, and 6.0 J/m². The equivalent free-air yield that would produce these energy fluxes at the same ranges may be derived using scaling laws from the 1 kt (nuclear) standard [ANSI S2.20, 1983]. The equivalent yields are: .0047, .0046, and 2.0 t(nuclear); after correcting for the 20% greater hydrodynamic energy release of ANFO compared to nuclear explosive these equivalent yields correspond to confinement factors of 2600, 3400, and 160 which may be compared to the factor of 1600 estimated simply on overpressure. This comparison neglects further energy loss at the shocks which would be experienced by free-air explosions during propagation to the ionosphere; such losses would be minimized for the smoother wave forms shown in Figure 3. These energy estimates indicate that the explosions in Figure 2 which were mostly of less than 10 t charge are well confined; more analysis is needed to discern whether there is a tendency for confinement to decrease with increasing explosion size.

3 Results

The major research issue of the first year of the EDIT project was the detectability of ionospheric perturbations produced by mining explosions. To address that question we deployed radio remote-sensing systems to monitor the ionosphere above two different mines: the Morenci copper mine in Arizona, and the San Juan coal mine in New Mexico. Our results indicate that we detected ionospheric signatures following known explosions at these mines consistent with those we would expect from airblast. In this section we discuss our measurement technique and the present a preliminary analysis of our data.

3.1 *Measurement Technique*

As discussed above, the airblast from mining explosions is much reduced compared to that produced by an unconfined explosion of the same yield; even large mining explosions will have an airblast equivalent to that produced by unconfined explosions with at most yields of a few tons. We have detected the airblast from unconfined explosions with yields of less than one ton using the sensitive technique of observing perturbations induced by acoustic waves on radio signals reflected from the lower ionosphere [Fitzgerald and Carlos, 1992]. We therefore decided to use this technique to monitor mining explosions. This technique, which has been applied by many

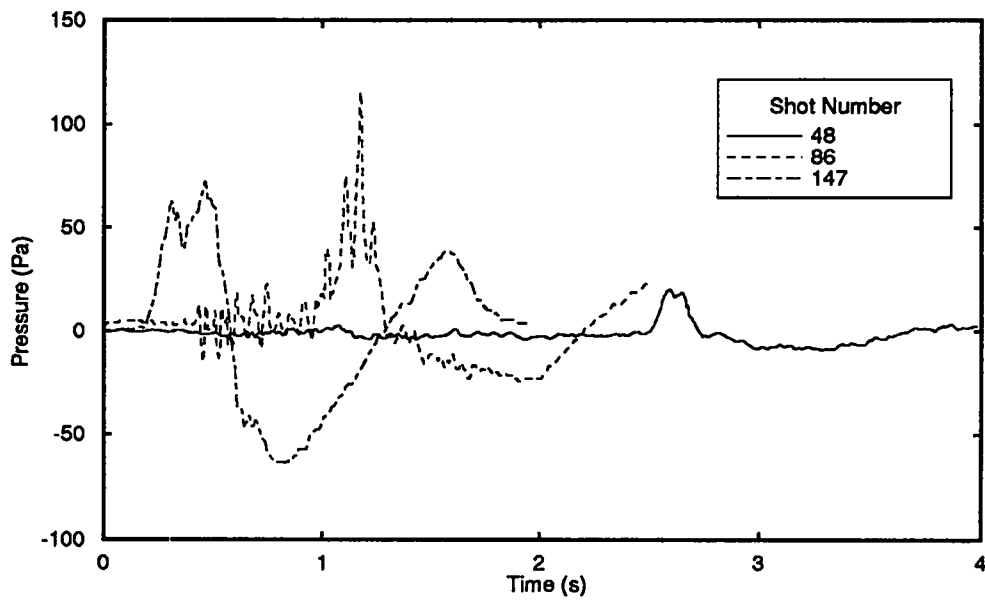


Figure 3: Measured pressure versus time for three mining explosions. Shot 48 was a 10.3 t detonation measured at a range of 741 m; shot 86 was 13.0 t at a range of 218 m; shot 147 was 262 t at a range of 2100 m [Siskind, et al., 1980].

researchers to detect acoustic waves produced by surface explosions, earthquakes, and underground explosions, relies on the fact that the reflection process is highly sensitive to small perturbations of the ionosphere near the reversal point. Moreover, it is relatively easy to reflect radio waves from the ionosphere using frequencies in one region of the electromagnetic spectrum. For simplicity, we designate this region the high frequency (hf) band which by definition covers frequencies between 3 and 30 MHz. Ionospheric reflection also occurs in the adjacent frequency bands: medium frequency (.3 to 3 MHz) and very high frequency (30 to 300 MHz) but is not the primary propagation mechanism as it is in hf band.

If one ignores the effect of the geomagnetic field, the index of refraction of the ionosphere for a radio wave of frequency, f , is $\sqrt{1 - f^2/f_N^2}$ where f_N is called the plasma frequency [Davies, 1990]. The plasma frequency is proportional to the square root of the electron density: $f_N^2 = Nc^2r_e/\pi$ where N is the electron density, c is the speed of light, and r_e is a constant (the classical electron radius). Using mks units, $f_N^2 \approx 81N$. A vertically propagating radio wave will be reflected at the altitude for which its index of refraction is zero; that is, the altitude for which $f = f_N$. The ionosphere, which is produced by the absorption of the high energy portion of the solar spectrum, forms a layer in the upper atmosphere beginning gradually near 90 km altitude and reaching a maximum electron density near 250 km altitude. The plasma frequency as a function of altitude up to the maximum may be measured by varying the frequency of the reflected radio wave and measuring the time of flight of the signal from the ground to the ionosphere and back to the ground. A typical daytime profile of altitude versus plasma frequency is shown in Figure 4; such profiles are subject to solar cycle, seasonal, diurnal, and shorter time scale effects. As can be seen from Figure 4, vertically incident radio waves with frequencies up to 8 MHz will be reflected from the ionosphere.

In our technique of remote monitoring of the ionosphere above a mine we use oblique propagation rather than vertical; that is, we locate a radio transmitter and receiver at spatially separated sites such that the mine is close to the mid-path. This geometry makes the reflection process sensitive to acoustic waves propagating directly from the explosion to the ionosphere. It can be shown that oblique propagation at a frequency, f , is equivalent with some restrictions to vertical propagation at a frequency of $f \cos \phi_o$ where ϕ_o is the angle of incidence of the ray upon the ionosphere [Davies, 1990]. That is, we can reflect at the same altitude in the ionosphere by increasing the frequency of our obliquely propagating radio transmission as we increase the separation our transmitter and receiver.

The transmissions that we use for monitoring explosions have high phase and amplitude stability; therefore, variations in phase and amplitude of the received signal arise from propagation effects among which the reflection process is the most important. A convenient way of displaying the time variations of the received signal is to plot the power spectrum of the complex amplitude versus time. That is, our received signal can be written as $a(t) \cos 2\pi ft$ where $a(t)$ is a complex time series. Our radio receiver and data analysis removes the $\cos 2\pi ft$ variation which contains no infor-

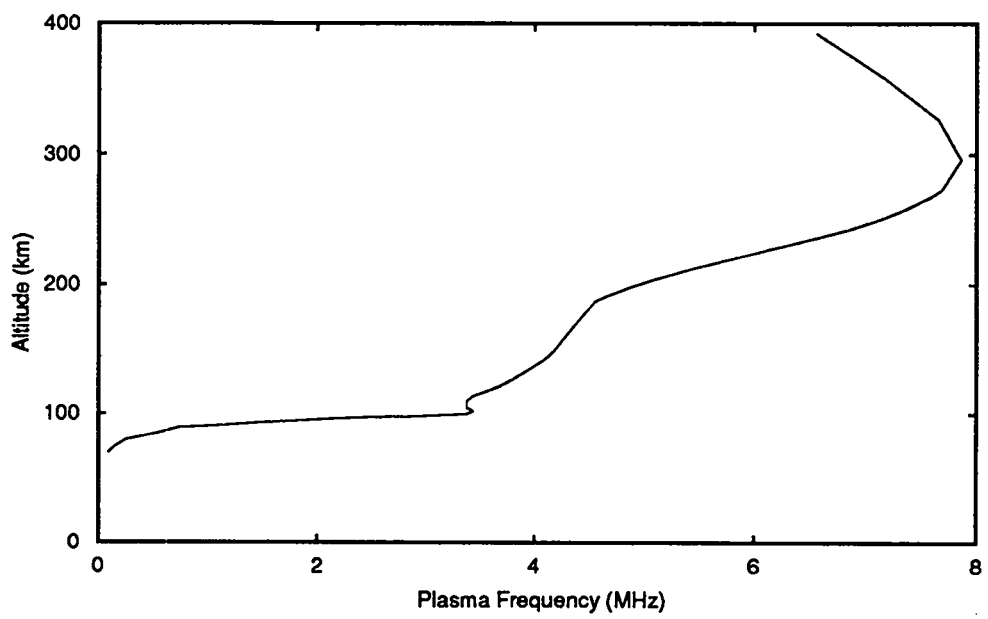


Figure 4: Typical profile of plasma frequency versus altitude; vertically incident radio waves will be reflected at the altitude for which the plasma frequency matches the frequency of the wave.

mation. Variations in the phase of $a(t)$ can arise from changes in the length of the propagation path; variations in the magnitude can arise from interference between multiple reflections, from focussing, and from variations in absorption. The time rate of change $a(t)$ is relatively slow so that power spectrum will usually show a peak near a frequency of 0 Hz. The type of change that we expect to be produced by acoustic waves from a small explosion is shown in Figure 5 where we plot a spectrogram of the complex amplitude versus time. This data was obtained near the Nellis Air Force bombing range in Nevada during an exercise during which there were multiple detonations of pairs of 500 pound bombs [Fitzgerald and Carlos, 1992]. Our interpretation of this data is that the explosions produced a hemispherically expanding shock wave which propagated up to the reflection altitude of our radio transmissions. The alteration of the electron density near the reflection altitude produced by the shock wave causes a temporary radio reflection via diffraction from the small perturbation. Because the intersection point of the shock wave and the reflection altitude changes in time, the temporary mode is offset in frequency; that is, the phase shows a variation in time. The offset is initially positive because the phase path shortens as the intersection point approaches the mid-path. At mid-path the offset goes to zero; then the offset becomes negative as the intersection point moves away from the mid-path and expands the phase path. We expect a similar signal from a mining explosion.

3.2 *Morenci Copper Mine*

We deployed an hf reflection system to monitor explosions at the large open pit copper mine near Morenci in south east Arizona. This system operated for a total of 15 days during January and May of 1993. The transmitters were located at Alpine, AZ, and the receivers at Bowie, AZ; their separation was 170 km (Figure 6). We transmitted at four frequencies to sample four altitudes in the ionosphere; we received the transmissions using two antennas spaced about 600 m apart. Table 3.2 lists the seismic events for which the difference in arrival times of the S and P waves are consistent with explosions at the Morenci Mine during the time that the radio systems were operating [Wallace, 1993]. The two largest events out of the five that occurred were detected; the largest event had a local magnitude, $m_L = 2.9$ [Wallace, 1993].

Figure 7 shows the spectrogram from one channel of data for the event of May 21. There is a brief broadening of the spectrum at about 300 s after the seismic origin time which we ascribe to an explosion at the Morenci mine. The time delay corresponds to the acoustic travel time to the lower ionosphere at about 100 km altitude. That altitude range is the likely reflection height of the 4.15 MHz transmissions recorded on this channel. A similar disturbance was also recorded on the signal received from the second antenna at the same frequency. A weaker disturbance was recorded a few seconds earlier than that shown in Figure 7 on the receivers monitoring the transmission at 3.55 MHz; since that transmission should have reflected at a slightly lower altitude, the origin of the disturbance is consistent with a vertically propagating acoustic wave. The brief duration of the disturbance points to a source almost directly

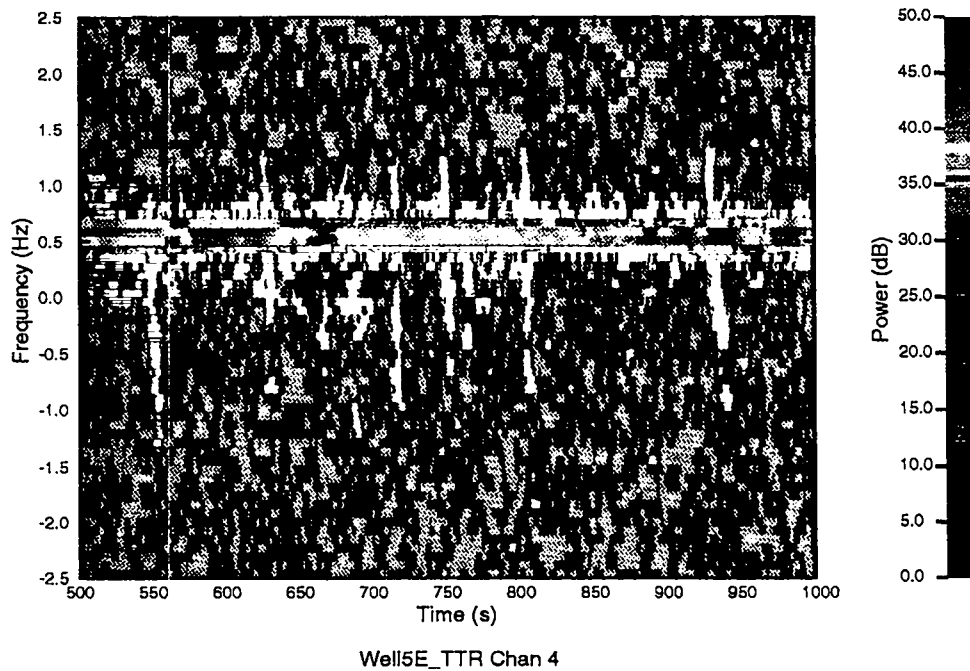


Figure 5: Spectrogram of received signal for a 3.82 MHz transmission between the Tonopah Test Range and Area 5 of the Nevada Test Site. The repeated broadening of the spectra resulted from multiple detonations of bombs during a training exercise at Nellis Air Force bombing range [Fitzgerald and Carlos, 1992].

Date	Time (UT)	Seismic Amplitude	Ionospheric Detection
Jan 29, 1993	18:00:10	1701	No
May 17, 1993	19:35:22	2904	Yes
May 18, 1993	22:14:07	2772	No
May 19, 1993	20:42:24	2154	No
May 21, 1993	19:15:17	4826	Yes

Table 1: Date and times of seismic events likely to have been explosions at the Morenci mine. The seismic amplitude is in arbitrary linear units.

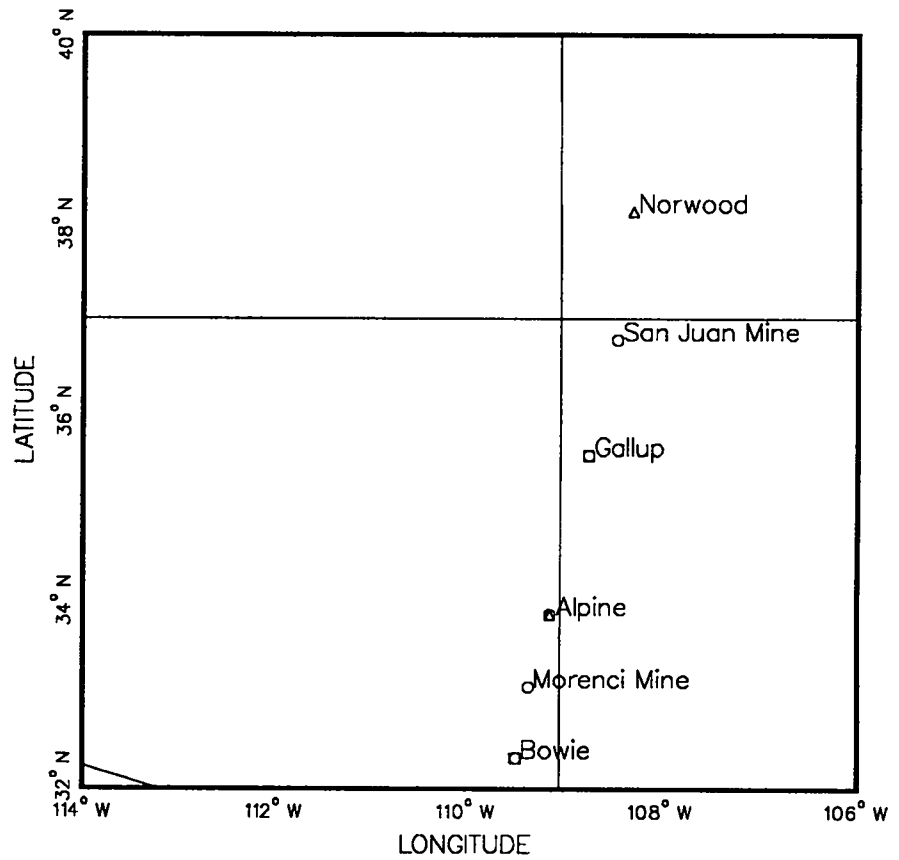


Figure 6: Map showing location of mines at San Juan, NM and Morenci, AZ; the transmit sites at Gallup, NM, and Alpine, AZ; and the receive sites at Norwood, CO, and Bowie, AZ.

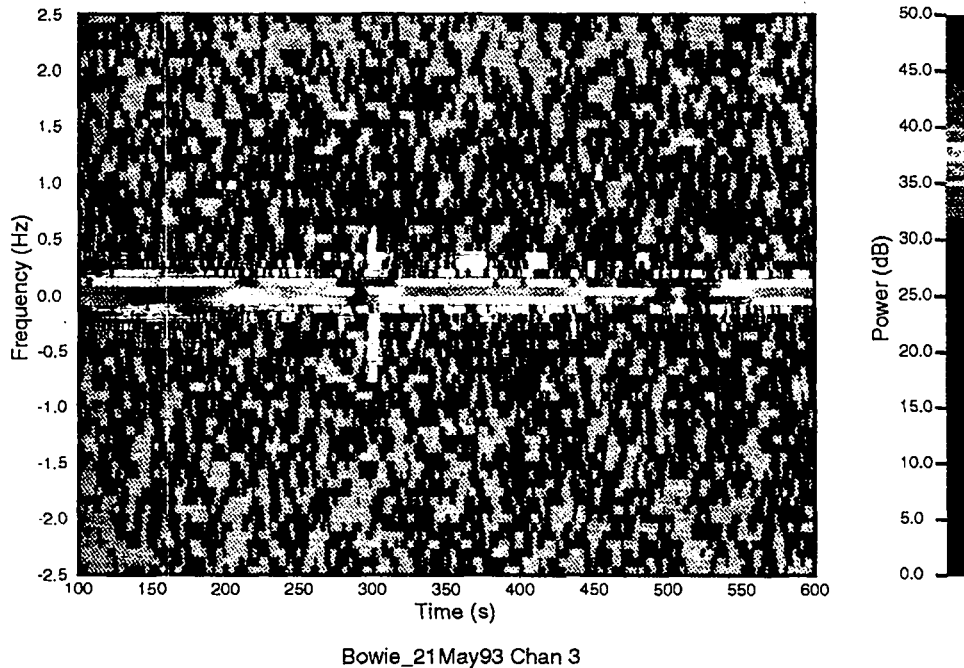


Figure 7: Spectrogram of received signal for the transmission at 4.15 MHz following the seismic event of May 21, 1993. Time is delay in seconds after the origin time. A disturbance consistent with an explosion source at the Morenci mine occurred at about 300 s.

below the ionospheric reflection point which was located above the Morenci mine. We would expect a behavior similar to that shown in Figure 5 for a more remote source; that is, the disturbance would start at positive frequency offset, move through zero, and proceed to negative offset. The time duration depends upon the distance of the source from the ionospheric reflection point because the apparent speed of the intersection point at which the scattering originates is greatest directly over the explosion and decreases with distance. The data from the two lowest transmission frequencies at 2.85 and 3.05 MHz did not show a disturbance.

The event of May 17 occurred at about the same time of day as that of May 21 but had a lower seismic amplitude. Figure 8 shows the spectrogram from the channel monitoring the 4.15 MHz transmission for the period from 100 to 600 s after the seismic origin time. There is broadening of the spectrum at about 300 s although the effect is weaker than that shown in Figure 7. The time delay and brief duration of

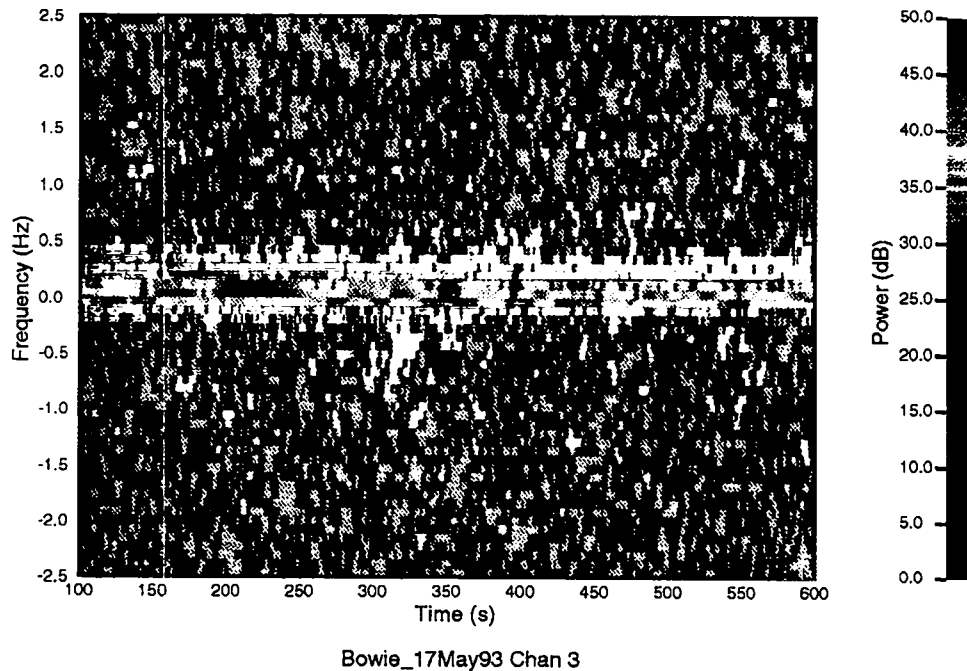


Figure 8: Spectrogram of received signal for the transmission at 4.15 MHz following the seismic event of May 17, 1993. Time is delay in seconds after the origin time. A disturbance consistent with an explosion source at the Morenci mine occurred at about 320 s.

the effect is again consistent with an explosion source at the Morenci mine. A similar disturbance was observed in the data for the same frequency from the other antenna. No disturbance was observed in the data from the lower frequencies at 2.85, 3.05, and 3.55 MHz.

There was no disturbance with the expected signature and the delay time on any of the transmission frequencies following the remaining three events that occurred during the time period monitored. As shown in Table 3.2 these events had lower seismic amplitude than the two for which there was an ionospheric detection.

3.3 *San Juan Coal Mine*

We redeployed the hf reflection system used to monitor the Morenci mine explosions to observe activity at the San Juan coal mine near Waterflow in north west New Mexico. This system operated during a time period in August, 1993, for which the

mine operators informed us that two large explosions would occur. The total charge for each of these explosions was expected to be about 1 kt. The transmitters were located at Gallup, NM, and the receivers at Norwood, CO; the separation was 290 km (Figure 6). We transmitted at five frequencies; we received the transmissions using two antennas spaced about 100 m apart.

The first of these two explosions took place on August 23, 1993; the origin time was identified as 23:05:13 UT from seismograph recordings obtained near Los Alamos, NM [House, 1993]. Figure 9 shows the spectrogram from the channel monitoring the 4.52 MHz transmission for the period from 100 to 600 s after the seismic origin time. There is broadening of the spectrum at about 340 s and again at about 460 s; we ascribe both of these effects to the mining explosion. Analysis of the data obtained at lower frequencies indicates that the 4.52 MHz transmission propagated via reflections at two altitudes in the ionosphere. Such multiple reflections are commonly observed for the oblique paths that we employ. It is likely that the lower reflection occurred at about 105 km altitude and produced the disturbance at 340 s; an upper reflection at about 140 km altitude would have produced a disturbance at about 460 s. A scan of frequencies obtained an hour after the explosion in which we identified reflection altitude via time delay of the propagation, indicates that multiple reflection was likely. The occurrence of a disturbance at the upper altitude indicates a relatively strong shock wave; typically weak shock waves suffer great dissipation between 100 and 140 km altitude. Disturbances were also detected at three lower frequencies: 3.52, 3.72, 3.92 MHz; no disturbance was detected at 2.52 MHz.

The mine operators informed us that the second explosion took place on August 29, 1993 between 20:20 and 20:25 UT; no seismograph records were obtained from Los Alamos to confirm the origin time. Figure 10 shows the spectrogram from the channel monitoring the 4.53 MHz transmission for the period from 100 to 600 s after 20:22:00 UT. There is broadening of the spectrum at about 325 s which we ascribe to the mining explosion. The intermittent broadening of the spectra that is observed during the 500 s period is broadband noise caused by lightning. A disturbance was also observed on data from the transmissions at 4.73 and 5.53 MHz; no disturbance was observed at 2.53 and 3.53 MHz.

4 Discussion

4.1 Detectability of Mining Explosions

Figure 11 plots the behavior of the seismic magnitude versus the total energy released as airblast for three types of sources: contained underground explosions, mining explosions, and single surface explosions. The curve for underground explosions is based on our measurements of nuclear tests at the Nevada Test Site; the curve for surface explosions is based on the observation that for low-yield surface explosions the seismic amplitude is about a factor of 10 lower than the same charge detonated in hard rock [Carpenter, 1967]. These curves indicate that a contained underground explosion with

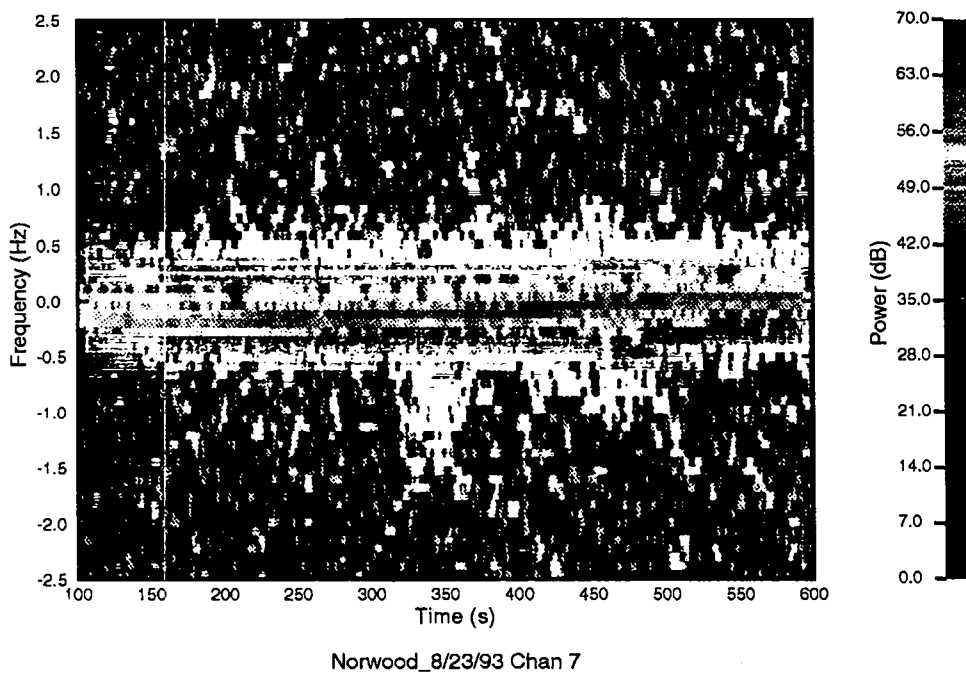


Figure 9: Spectrogram of received signal for the transmission at 4.52 MHz following the explosion at the San Juan mine on Aug 23, 1993. Time is delay in seconds after the origin time. A disturbance occurred at about 340 s and again at 460 s which we ascribe to the explosion. The occurrence of two disturbances probably results from reflection at two separate altitudes in the ionosphere.

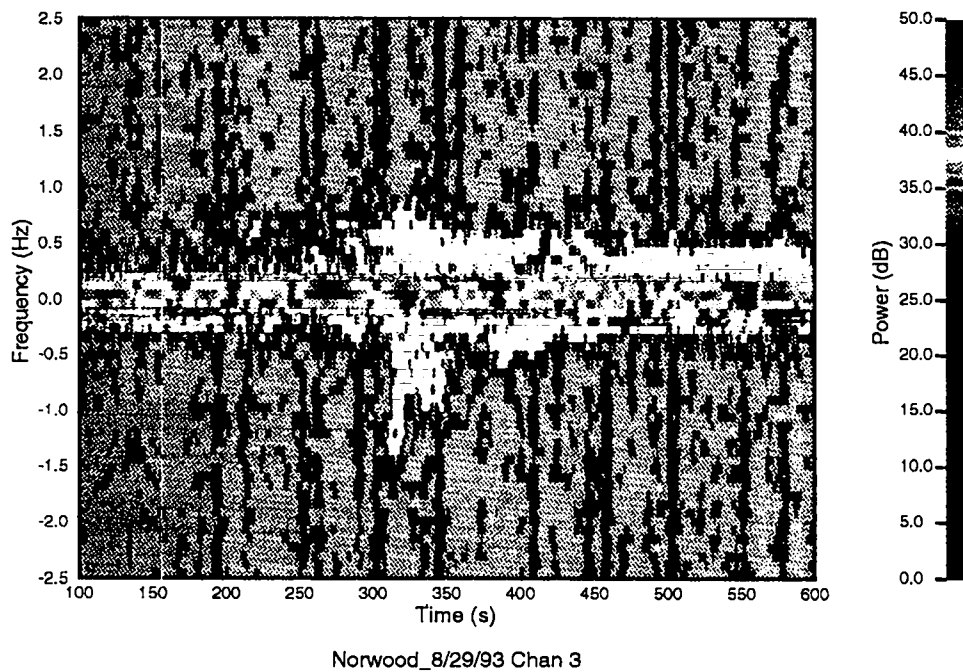


Figure 10: Spectrogram of received signal for the transmission at 4.53 MHz following the explosion at the San Juan mine on Aug 23, 1993. Time is delay in seconds after 20:22 UT, the approximate origin time. A disturbance occurred at about 325 s which we ascribe to the explosion.

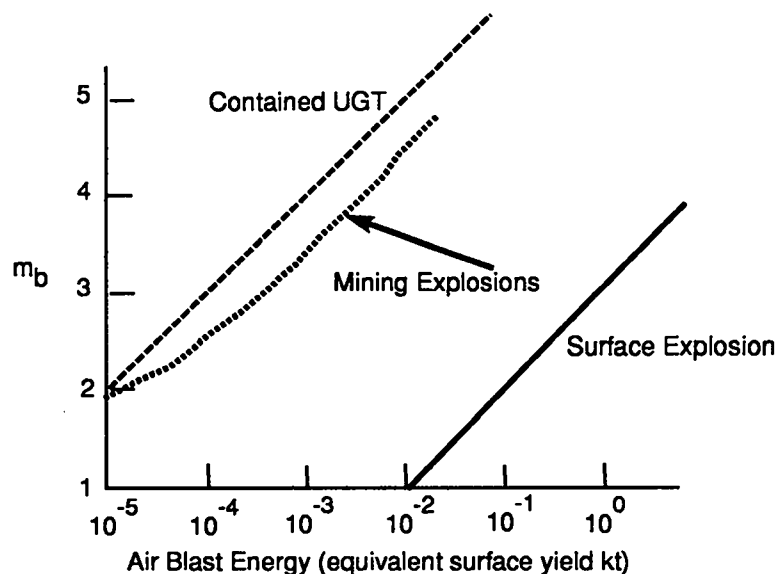


Figure 11: Plot of seismic magnitude versus effective airblast energy for three types of sources: fully tamped underground explosions, surface explosions, and mining explosions.

a seismic magnitude of $m_b = 4$ releases the same airblast as a 1 ton surface explosion; on the other hand, a 1 kt surface explosion would have a seismic magnitude of 3 using the scaling that $m_b \approx 4$ for a well coupled 1 kt underground explosion. The curve labelled mining explosions is based on the detectability of the Minnesota seismic array for earthquakes and mining explosions [Greenhalgh, 1980]; it also assumes a factor of 400 for the containment of larger mining explosions.

The curve for mining explosions in Figure 11 is a rough estimate and needs to be verified by measurements; it appears to approximately represent the position of the May, 1993 data described above. However, the curves indicate that there is a significant difference in energy released as airblast between contained underground explosions and mining explosions of the same seismic magnitude. This difference could serve as a discriminant: a seismic event of magnitude three with an intermediate airblast would be classified as a mining explosion; an event with a large airblast would be classified as an uncontained explosion. If little or no airblast were detected then the event would be suspect.

4.2 System Concepts

One possible ionospheric detection method would be to monitor satellite beacon transmissions; for example, global positioning satellites (GPS) transmit at a frequency of about 1.4 GHz. The ionosphere is transparent at that frequency but one can determine the column density of electrons along the path from the satellite to the receiver (total electron content or TEC) using special receivers. If the acoustic perturbation

from an explosion intersects this path it will change the electron density in a limited region and thus the integrated column density. Typical TEC values range from 10^{16} to 10^{18} m^{-2} . Measurements from a .5 t surface explosion indicate that we can expect a perturbation of about 1 % in electron density in the lower ionosphere [Fitzgerald and Carlos, 1992]. Given an ambient density of 10^{11} m^{-3} and a path length in the perturbation of 10 km then the change in TEC would be 10^{13} m^{-2} ; the sensitivity of GPS systems is about 10^{14} m^{-2} so that the perturbation would be below the threshold of detectability.

Given the lack of sensitivity of the transionospheric scheme, a possible monitoring system could be based on an adaptation of the ionospheric reflection technique. For example, one could monitor the carrier of ordinary shortwave radio broadcasts which employ amplitude modulation to transmit voice and music. The spectrum of such broadcasts consists of a carrier at the transmit frequency and sidebands of a few kHz width which contain the amplitude information. Our receivers which have a narrow band filter of less than 100 Hz width may be tuned to receive only the carrier and eliminate the sidebands containing the modulation. Our detection technique looks for changes of a few Hz in the carrier which is below the lowest frequency of the modulation passband. Thus the shortwave broadcasts may be treated as beacons and need not be cooperative. Such a concept is illustrated in Figure 12 which shows paths between hf broadcast stations in North Korea and a receiver station in South Korea. Each path will be sensitive to disturbances originating near its mid-point; the numbers indicate the broadcast frequency in kHz [Sennitt, 1993]. Greater areal coverage could be gained by adding more receiver stations and by monitoring transmissions from China or Russia. The cost of a receiver station capable of monitoring 10 transmissions would be about \$100,000.

5 Conclusion

We detected the airblast from four mining explosions using radio techniques to remotely monitor the ionosphere above the mines. The ionospheric signatures were consistent with the confinement factors determined from local measures of airblast which indicate that for most mining explosions the energy released as airblast is less than 1% of that released for an single unconfined explosions of the same total charge.

Some of the smaller monitored explosions were not detected using our techniques. This indicates that the airblast associated with these explosions is weak and dissipates before it reaches the ionosphere. Local airblast measurements indicate that smaller explosions are more confined than larger explosions. Our results also indicate that lowest radio frequencies that we employed were not as effective in detection as the higher frequencies. Broadband noise generated by lightning also causes interference with our detection process; this effect would be mitigated if we employed higher frequencies necessary when the transmitters are located at greater range from the explosion. Noise caused by lightning falls off dramatically with increasing frequency.

Future effort on the EDIT project will be directed at increasing the data base

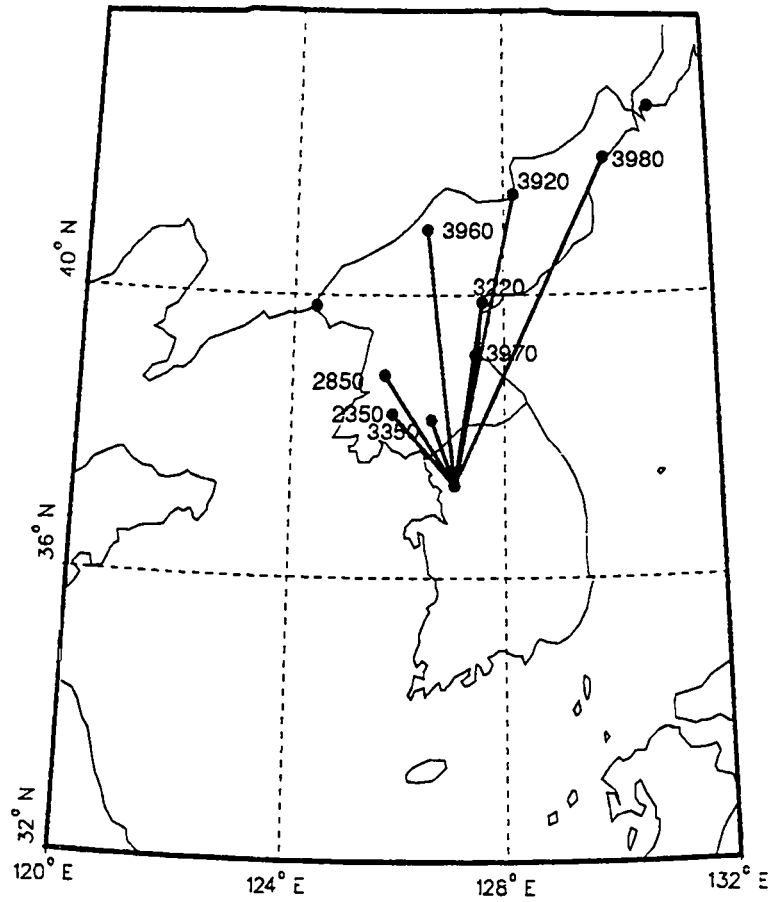


Figure 12: Map showing radio propagation paths from broadcast stations in North Korea to a receive site in South Korea. The frequencies of the broadcast in kHz are indicated near their origin. Each path would be sensitive to explosions originating near its mid-point.

of monitored mining explosions; our goal is to characterize the detectability of such explosions using the hf reflection technique in relation to the seismic magnitude scale. That will allow us to determine the usefulness of ionospheric discrimination in a total monitoring system including seismic. In order to monitor more explosions we will automate our data acquisition fully to allow continuous operation under computer control. Such automated data acquisition would be a prototype for a deployable system. We will also extend the baseline between our transmitters and receivers so that we operate at regional ranges of 500 km from the explosion; this will give us experience at difficulties that might be encountered using longer range radio propagation.

6 Acknowledgement

This work was performed under the auspices of the U. S. Department of Energy by Los Alamos National Laboratory under contract W-7405-ENG-36. We would like to thank Terry Wallace of the University of Arizona and Lee House of Los Alamos National Laboratory for making available their seismic data.

7 References

ANSI S2:20, *American National Standard: Estimating Airblast Characteristics for Single Point Explosions in Air*, American Institute of Physics, New York, 1983.

Carpenter, E. W., Teleseismic signals calculated for underground, underwater, and atmospheric explosions, *Geophysics*, 32, 17-32, 1967.

Davies, Kenneth, *Ionospheric Radio*, Peter Peregrinus, 1990.

Greenhalgh, S. A., H. M. Mooney, and C. C. Mosher, The Minnesota seismic network, *Bull. Seismo. Soc. Am.*, 70, 1347-1368, 1980.

Fitzgerald, T. J., and R. C. Carlos, The effects of 450 kg surface explosions at the E layer of the ionosphere, *Rept. LAUR-92-3393*, Los Alamos National Laboratory, Los Alamos, NM, October, 1992.

House, L. S., Los Alamos National Laboratory, personal communication, 1993.

Morhard, Robert C., *Explosives and Rock Blasting*, Atlas Powder Company, Dallas, TX, 1987.

Richards, P. G., D. A. Anderson, and D. W. Simpson, A survey of blasting activity in the United States, *Bull. Seismo. Soc. Am.*, 82, 1416-1433, 1992.

Sennitt, A. G., ed., *World Radio TV Handbook*, Billboard Books, 1993.

Siskind, David E., Vibration criteria for surface mine blasting: ten years after Bureau of Mines RI 8507, *Proc. Symposium on Explosives and Blasting*, Society of Explosives Engineers, 1990.

Siskind, D. E., V. J. Stachura, M. S. Stagg, and J. W. Koop, Structure response and damage produced by airblast from surface mining, *Rept. RI 8485*, Bureau of Mines, U. S. Department of the Interior, 1980.

Wallace, T., University of Arizona, personal communication, 1993.

UNIVERSITY OF ARIZONA
LIBRARY

LOS ALAMOS NAT'L LAB.
IS-4 REPORT SECTION
RECEIVED

'94 FEB 18 AM 7 51